Effect of decomposition temperature on crystallite size and strain of CaO

Sattar A. Abass, Abass F. Almamori and Amel D. Hussain

Physics Department, College of Science, Waist University, Iraq.

ABSTRACT

The crystallite size and strain of CaO ceramic powder have been determined from X-ray line-broadening analysis at different decomposition temperatures. The CaO powder has been prepared from decomposition of calcium carbonate $CaCO_3$ at different temperature which have been characterized by X-ray diffraction (XRD) and Differential, Thermal Analysis (TG, DTA) methods. Correction of the FWHM by Warren – method has resulted in corrected values of crystallite size. The crystallite size has been found to increase with increasing decomposition temperature from 30.2 nm at 800°C to 58.7 nm at 1200°C. Strain on the other hand decreases from 2.89×10^{-3} at 800°C to 1.53×10^{-3} at 1200°C. Estimation of micro hardness on compacts of different crystallite sizes has showed that crystallite size may influence the bearing load that compact can endure.

Keywords: X-ray diffraction, crystallite size, materials, heat treatment.

*Corresponding author. E-mail: boshera65m@yahoo.com.

INTRODUCTION

Calcium minerals have been used extensively in the food preparation and in steel industry and in the petrochemical industry, plastics fine chemicals, manufacturing of additives to oils, protective surface on metal and boards, and in water treatment.

Calcium oxide is usually produced by calcining $CaCO_3$ above 800°C. The reactivity of the produced CaO depends on the calcinations temperature, and above 1100°C it is in the unreactive form which is used as basic in manufactures (Whaley, 1981; Worral, 1998; Driscoll, 1985; Maass et al., 1999; Pajunen, 2001; Huang et al., 2005; van Dijk, 2011).

Determination of the crystallite size and morphology of CaO prepared by calcinations of calcium carbonate, made by use of X-ray diffraction method has shown that crystallite size extend over a range of values from 40 to 150 nm and the morphology of the decomposed product is similar to that of the parent compound (Jones et al., 1980). The present investigation aimed to calculate crystallite size, strain from decomposed calcium carbonate, and to show if these have any influence on the hardness properties.

EXPERIMENTAL

To characterize the reactants and their decomposition, different techniques were used. They were the automated X-ray powder diffraction system for recording diffraction pattern with copper K_α radiation ($\lambda = 0.15406\,nm$). In addition to the necessary treatment on the scanned peaks, the TG system for recording TG and DTA curves under controlled atmospheres, heating rate of 20°C/min and $\propto$- alumina was used as reference material for DTA. Assessment of mechanical properties of powder compacts by Vickers micro hardness was made with applied load of 100 g and square diamond pyramid with opposite faces at 136°.

Analysis of line breath

The extent of line breadth was taken as a measure due to small-crystallite of CaO powders. Measurements were based on the FWHM (Full Width at Half Maximum) of five diffraction lines namely (111), (200), (202), (311) and
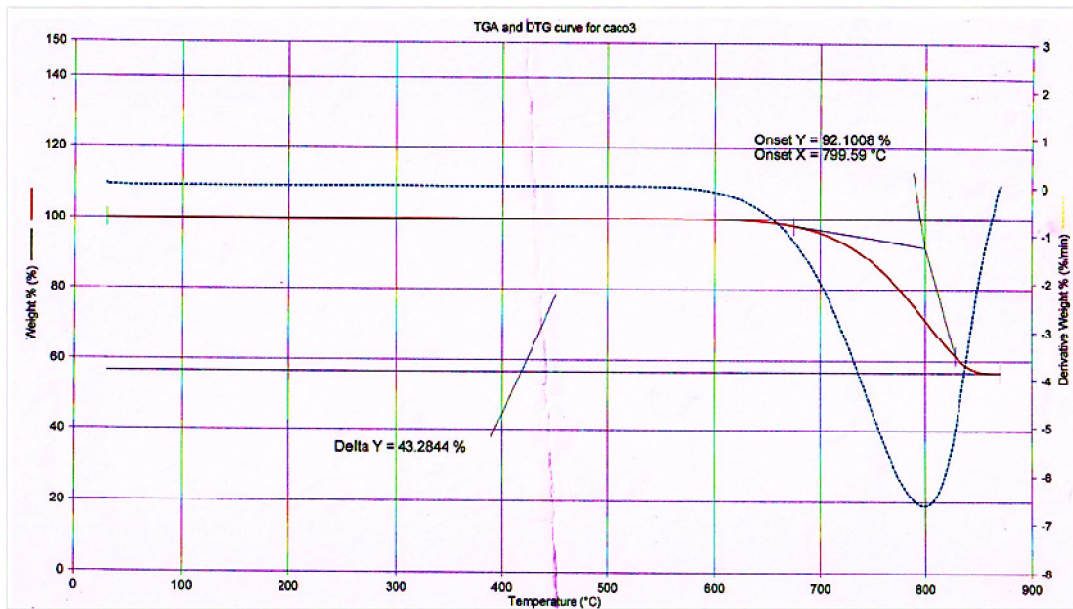
Figure 1. TG curves as recorded for $CaCO_3$.

(222). Two most commonly assumed line shapes are the Cauchy and Gaussian functions. For Cauchy profile, originally analysis of crystallite size effects, the correct crystallite size breadth is given by (Stokes, 1948):

$$\beta_{cs} = \beta_{meas} - \beta_{instr} \tag{1}$$

Where $B_{meas.}$ is the experimentally measured breadth and $B_{instr.}$ is the half width of the instrumental breadth. For Gaussian profile, which is more correctly represent the actual reflection profile and instrumental Profile, Warren suggested the relation for the correct size (Azaroff, 1968) as:

$$\beta^2_w = \beta^2_m - \beta^2_i \tag{2}$$

The relationship is holding for both-maximum and integral breadths. Since the actual profiles are never pure Gaussian or pure Cauchy. These simple formulae have only limited practical value. In the absence of clear-cut evidence whether the Scherrer relation (1) or Warren relation (2) should be used, also Warren suggested a formula that take into account the geometric mean as:

$$\beta_{WC} = [(\beta_{meas.} - \beta_{instr.})(\beta^2_{meas.} - \beta^2_{instr.})^{1/2}]^{1/2} \tag{3}$$

The crystallite size and strain can be calculated from formula (De Keijser et al., 1982). When certain line shape is assumed such as Gaussian or Cauchy functions:

$$L_{cs} = \frac{K\lambda}{\beta_{WC}\cos\theta} \tag{4}$$

$$\epsilon = \frac{\beta_{cs}}{4\tan\theta} \tag{5}$$

Where L_{cs} is the crystallite size, λ is the wavelength of the radiation, β_{wc} is the corrected breadth (in radians), θ is the Bragg angle, K is the Scherer constant whose value $2(In2/\pi)^{1/2}=0.94$ (Warren, 1969), and (ϵ) is the strain.

RESULTS AND DISCUSSION

Characterization of starting material

Figures 1 and 2 show TG and DTA curves for decomposition of $CaCO_3$ in helium and argon atmosphere, respectively. It can be seen from the TG curve that the decomposition begins around 662°C and continues progressively to about 900°C with inflection at 799.59°C. The composition of various residues left after complete decomposition under controlled atmosphere is determined by decomposition analysis. Results are presented in Table 1.

The DTA curves in Figure 2 show one endothermic sharp peak at about 800°C corresponding to loss of carbon dioxide and found small sharp at about 370°C corresponding to hydrate in water. Above 1100°C in the decomposition curve, all the samples showed characteristic CaO patterns. These data agree well with those cited by Stanmore and ilot (2006) and Tang (2013).

Figure 3 shows the X-Ray diffraction pattern of calcite powder at room temperature. Table 2 summarizes the
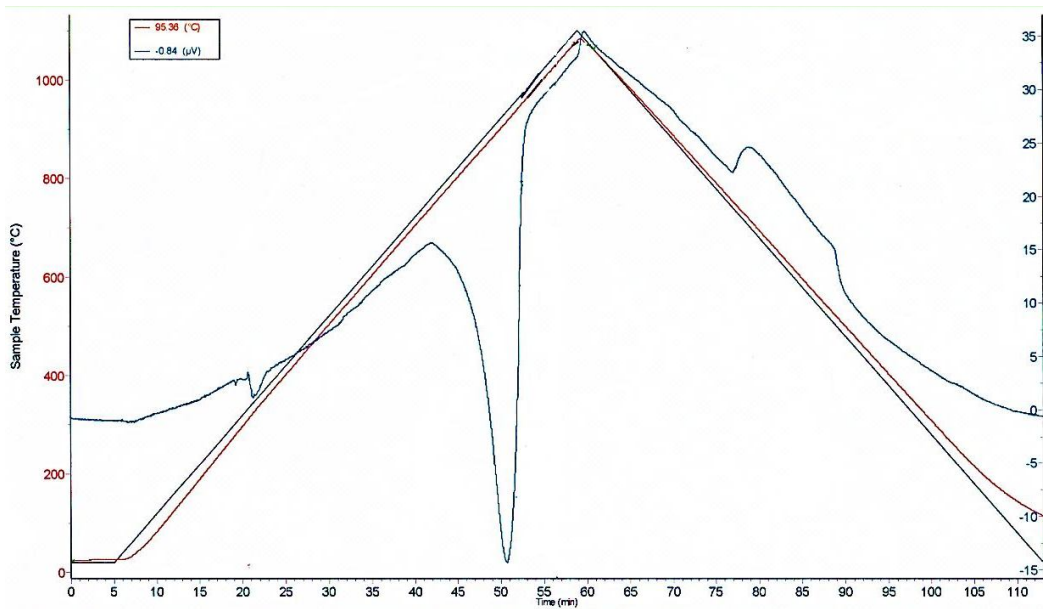
Figure 2. DTA curves as recorded for $CaCO_3$.

Table 1. Decomposition analysis for calcium carbonate.

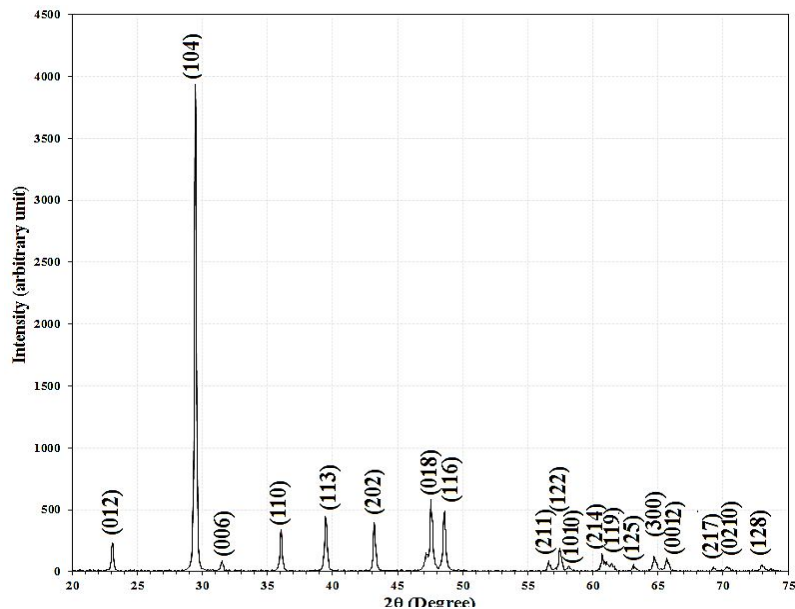| Parameter	Starting compound	Lost compound		Residual compound	
Chemical formula	$CaCO_3$	CO_2		CaO	
Molecular weight	100	44		56	
Weight	Initial weight	Lost weight measured	Lost weight calculated	Residual weight measured	Residual weight calculated
	59.244 mg	25.935 mg	26.062 mg	33.236 mg	33.1766 mg
Molarities	0.5924	0.5894		0.5924	0.5894

Figure 3. X-ray diffraction patterns of $CaCO_3$ at room temperature.

Table 2. Structural parameters viz. inter-planar spacing, crystalline size of pure CaCO$_3$.

2θ Exp (Deg.)	2θ Std (Deg.)	d$_{hkl}$ Exp. (Å)	d$_{hkl}$ Std. (Å)	I/I$_1$ Exp	I/I$_1$ Std	hkl
23.1504	23.021	3.8389	3.860	6	12	(012)
29.4905	29.404	3.02646	3.0357	100	100	(104)
31.5063	31.416	2.8373	2.8450	2	3	(006)
36.0563	35.964	2.48898	2.4950	9	14	(110)
39.4864	39.399	2.28031	2.2850	12	18	(113)
47.5871	47.487	1.90932	1.9129	16	17	(018)
48.5911	48.510	1.87219	1.8750	14	17	(116)
56.5900	56.551	1.6251	1.6260	4	4	(211)
57.4678	57.398	1.60231	1.604	5	8	(122)
58.1241	58.071	1.5858	1.5870	2	2	(1010)
60.7271	60.674	1.52388	1.5250	4	5	(214)
61.4226	61.341	1.5083	1.510	4	3	(119)
63.1102	63.056	1.4720	1.4730	2	2	(125)
64.7271	64.674	1.43916	1.440	3	5	(300)
65.642	65.594	1.4212	1.4220	4	3	(0012)
69.247	69.226	1.3557	1.3560	1	1	(217)
70.321	70.233	1.3376	1.3390	2	2	(0210)

a = 4.98, c = 17.06. CAS Number: 13397-26-7.
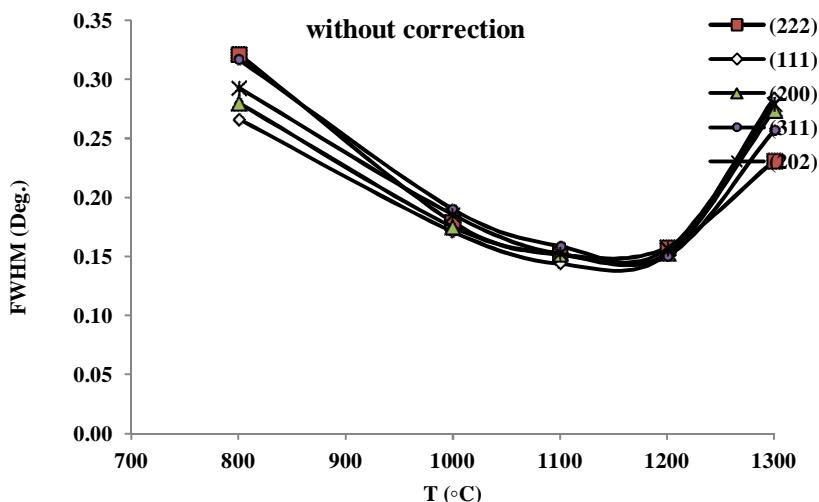
Figure 4. FWHM with temperature without correction.

experimental data observed for data observed for this powder along with the International Centre for Diffraction Data ICDD, compared with Card No. 13397-26-7 for CaCO$_3$ (Powder Diffraction File, 1997). It can be seen that the result of d-spacing and I/I$_0$ agree within acceptable variation of 5 and 10% with each other respectively. The decomposition analysis and XRD results confirmed the composition is CaCO$_3$ material. The decomposition analysis and XRD results confirmed the composition is CaCO$_3$ material.

Figures 4, 5, 6 and 7 show the variation of the FWHM without correction, with Scherrer correction and Warran (1969). Corrections with decomposition temperature for CaO from calcium carbonate. For the five reflections (111), (200), (202) (311) and (222), the half width decreases sharply up to 1050°C and slowly up to 1200°C. At higher temperature (1200 to 1300°C) the FWHM increases with temperature due to some variations in the crystallinity behavior of CaO depending on the crystallographic direction and morphology. These values obtained in this work are in agreement with literature (Danilchenko et al., 2006; Nirmala and Suresh, 2013).
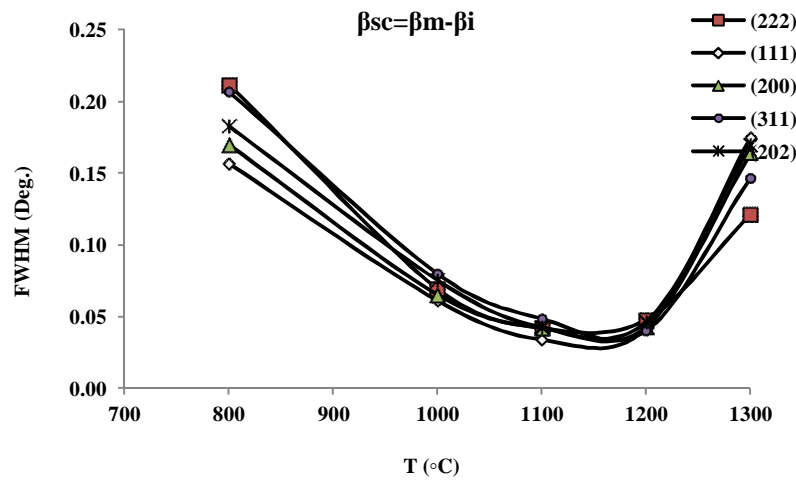
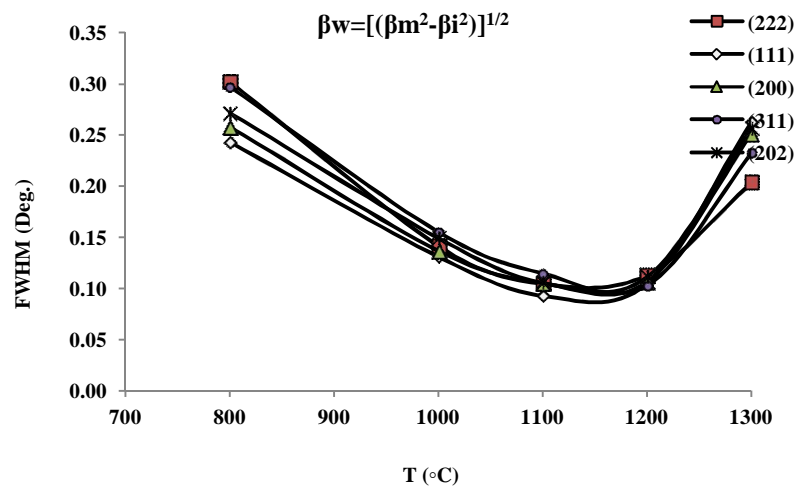**Figure 5.** FWHM with temperature with instrument correction.

Figure 6. FWHM with temperature with Warren correction (Warren, 1969).
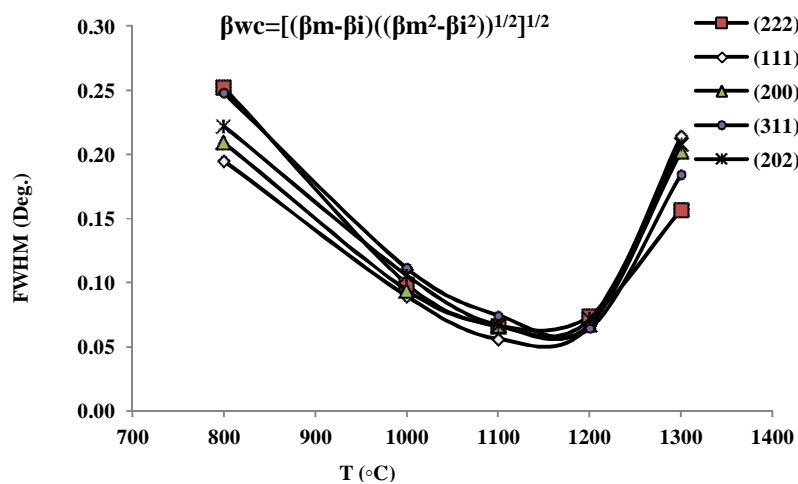

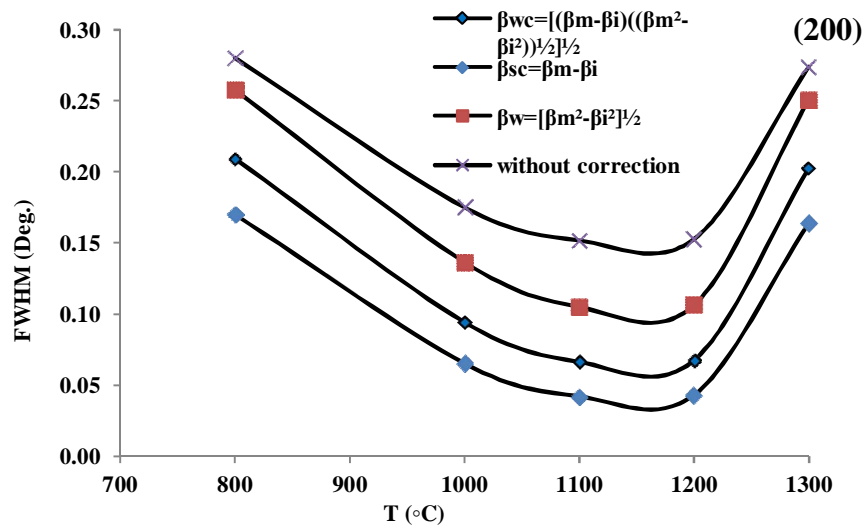**Figure 7.** FWHM with temperature with Warren correction (Warren, 1969).

Figure 8. Variation of FWHM with decomposition temperature for different correction methods for (200) reflection.
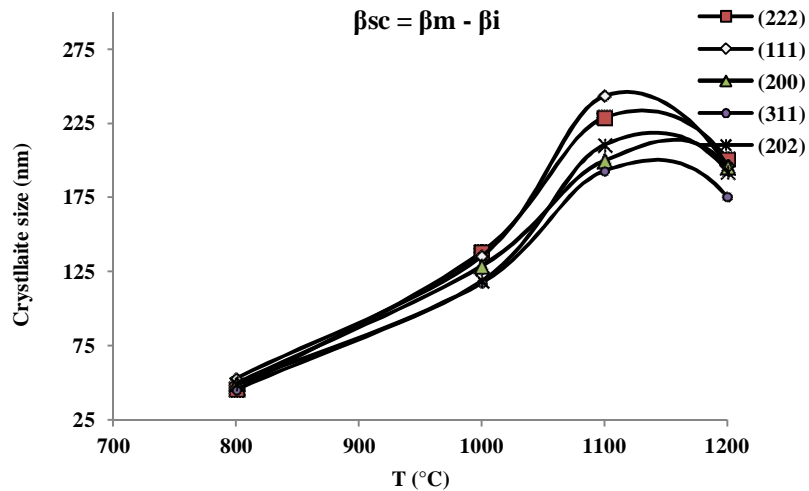

Figure 9. Crystallite size of CaO in nm for different temperature from $CaCO_3$ by Scherrer's method.

Therefore, we choose this method for comparison between uncorrected FWHM and the corrected FWHM by Warren – corrected method (Warren, 1969).

Figure 8 shows the variation of FWHM with decomposition temperature for the three methods of correction together with decomposition temperature for the three methods of correction together with the uncorrected FWHM for CaO. The 200 reflection has been taken as a representive example only. The FWHM for all curves have the same behavior. It appears that the temperature has significant effect on the FWHM especially at low temperature when the conversion is at its beginning and has a little effect at higher temperature.

It is also noticed that the curve in the Warren's corrected method has values in between the Warren's and Scherrer methods.

Figures 9 and 10 show the variation of crystallite size with decomposition temperature. Temperature has significant effect on the crystallite sizes and strain of CaO irrespective of the starting materials. As the temperature increases, the size of the crystallites perpendicular to (111), (200), (202) (311) and (222) reflections increases steadily from 800°C to about 1200°C; and after 1200°C the crystallite size decrease due to change of FWHM in this range. The inverse behavior is observed for strain. The crystallite sizes and strain values obtained in this
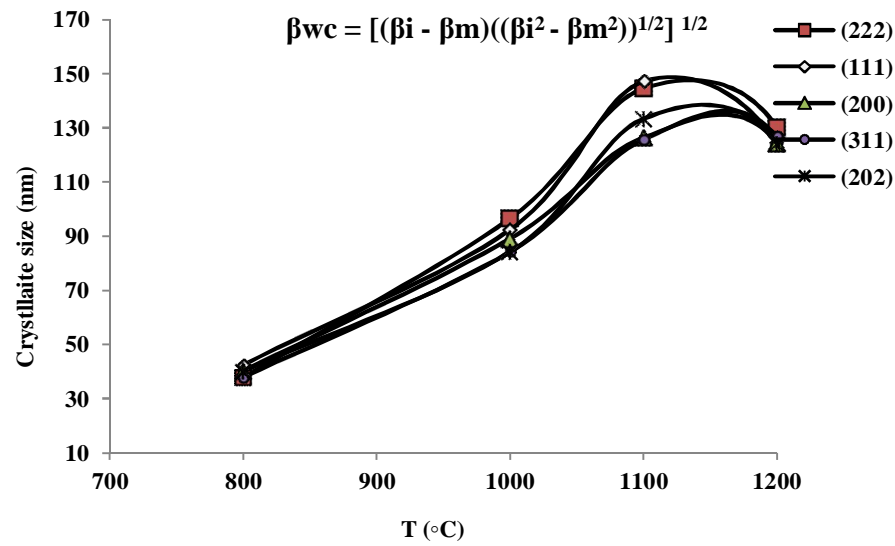
Figure 10. Crystallite size of CaO in nm for different temperature from $CaCO_3$ (Warren's correction method) materials.

Table 3. Crystallite size and R.M.S. strain as calculated by Warren correction for $CaCO_3$ yielded from thermal decomposition of $CaCO_3$.

Reflection hkl	Temperature (°C)	Crystallite size (nm)		R.M.S. Strain $\times 10^{-3}$	
		Without correction	With Warren corrected	Without correction	With Warren corrected
111	800	31.0	42.4	4.0153	2.9371
	1000	48.3	92.2	2.5741	1.3462
	1100	57.5	147.2	2.1614	0.8437
	1200	54.4	124.4	2.2767	0.9954
200	800	30.0	40.1	3.6037	2.6927
	1000	47.9	89.0	2.2523	1.2122
	1100	55.2	126.4	1.9499	0.8515
	1200	54.9	124.3	1.9567	0.8638
202	800	30.5	40.1	2.5079	1.9071
	1000	48.1	84.1	1.5871	0.9076
	1100	58.5	133.4	1.3033	0.5719
	1200	57.0	124.2	1.3352	0.6132
311	800	29.6	37.8	2.2018	1.7229
	1000	49.4	84.3	1.3196	0.7732
	1100	59.1	125.7	1.1007	0.5177
	1200	62.4	126.7	1.0424	0.4467
222	800	29.7	37.8	2.1013	1.6521
	1000	53.3	96.6	1.1702	0.6461
	1100	63.0	144.5	0.9901	0.4313
	1200	60.6	130.2	1.0272	0.4782

work are in agreement with those for CaO, MgO, ZnO, MnO_2 found in Acfarya and Pradhan (1986), Musa (1999) and Zhu et al. (2011).

The crystallite sizes at different temperatures were determined from the Scherrer and Warran correction. The results are shown in Table 3 with crystallite size for (111),
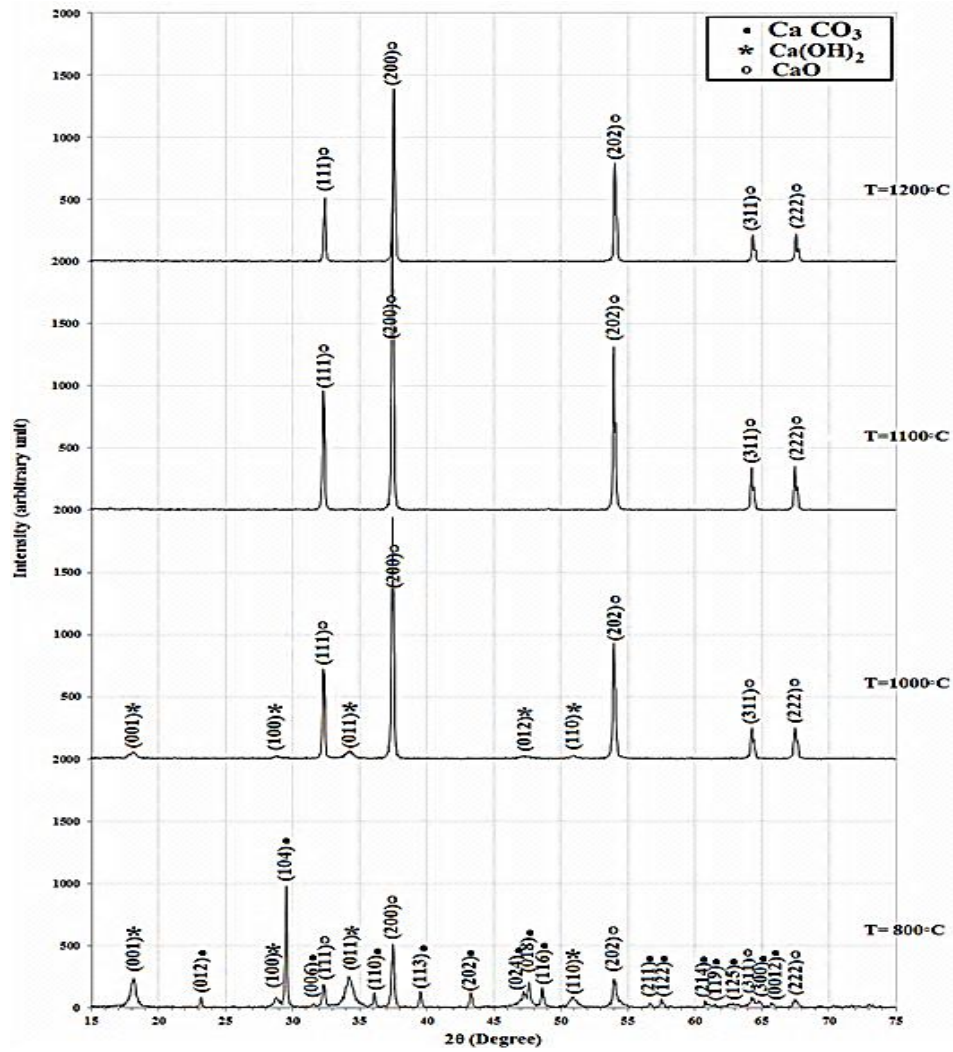
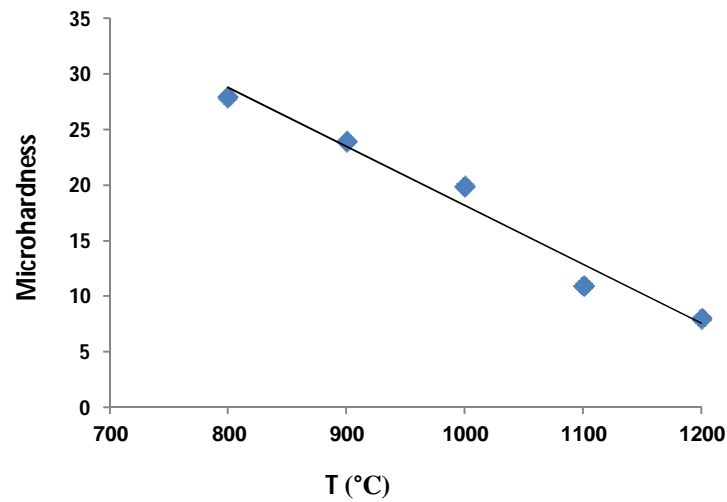**Figure 11.** Diffraction of CaO at 800, 1000, 1100 and 1200°C.

Figure 12. Vickers hardness number of CaO derived from CaCO$_3$ at 800, 900, 1000, 1100 and 1200°C.

(200), (202), (311) and (222) reflection as well. The different sizes with respect to different reflections indicate the anisotropic nature of the crystallites in these directions. Figure 11 shows the thermal decomposition for $CaCO_3$ at 800, 1000, 1100 and 1200°C.

Figure 12 shows the Vickers micro hardness number of CaO powder compacts depend on the crystallite size determined at certain temperature with the lower crystallite size of 30.2 nm having higher hardness number of 28 and higher size of 58.7 nm having hardness number of 11. This means that compacts made from higher finer powders endure better loads.

REFERENCES

Acfarya BS, **Pradhan** LD, **1986**. Determination of crystallite size and strain in γ-manganese dioxide - an X-ray diffraction study. J Appl Cryst, 19:214-216.

Azaroff IV, **1968**. Elements of X-Ray Crystallography. McGraw-Hill Book Company.

Danilchenko SN, Koropov AV, Protsenko IY, Sulkio-Cleff B, Sukhodub LF, **2006**. Thermal behavior of biogenic apatite, an x-ray diffraction study. Cryst Res Technol, 41(3):268-275.

De Keijser TH, Langford JI, Mittemeijer EJ, Vogels ABP, **1982**. Use of the Voigt function in a single-line method for the analysis of X-ray diffraction line broadening. J Appl Cryst, 15:308-314.

Driscoll DJ, Martir W, Wang JX, Lunsford JH, **1985**. Formation of gas-phase methyl radicals over magnesium oxide. J Am Chem Soc, 107:58-63.

Huang L, Li D, Lin Y, Wei M, Evans DG, Duan X, **2005**. Controllable preparation of Nano-MgO and investigation of its bactericidal properties. J Inorganic Biochem, 99:986–993.

Jones CF, Segall RL, Smart RSC, Turnera PS, **1980**. Correspondence: Size distribution of MgO smoke particles. Phil Mag A, 42:267-270.

Maass P, Meyer M, Bunde A, **1999**. Percolation effects in mixed β/β″-alumina crystals. Physics A, 266:197-202.

Musa SM, **1999**. M. Sc. Thesis University of Baghdad.

Nirmala PN, **Suresh** G, **2013**. Influence of the particle size on the optical properties of CaO thin film. Int J Recent Sci Res, 4(9):1320-1322.

Pajunen P, **2001**. P. Eng. Eco-Tec inc. AEC 2001 Finishing work shop.

Powder Diffraction File, **1997**. Alphabetical Index. Inorganic Compounds published by the, JCPDS. International Center for Diffraction Data U.S.A. v.1.30.

Stanmore BR, **Ilot** PG, **2006**. Review—calcination and carbonation of limestone during thermal cycling for CO_2 sequestration. Process Technol, 86: 1707-1743.

Stokes AR, **1948**. A numerical fourier-analysis method for the correction of widths and shapes of lines on x-ray powder photographs. Proc Phys Soc, 61:382-390.

Tang Z, **2013**. Sonication – assisted preparation of CaO nanoparticles for antibacterial agents. Quim Nova, 36(7):933-936.

van Dijk M, **2011**. Steel production, Cement production, non-ferrous metal production. a Quality Control Analyst Almatis Rotterdam Laboratory.

Warren BE, **1969**. X-Ray Diffraction. Addison-Welsiey. p. 251-314.

Whaley TP, **1981**. "Speciality Inorganic chemicals", ed by Thomson, pp. 122-163..

Worral WE, **1998**. L2m Construction chemicals, Inc. Grib it and Grib it AO, non. Slie aluminium oxide floor treatment.

Zhu Y, Wu S, Wang X, **2011**. Nano CaO grain characteristics and growth model under calcinations. Chem Eng J, 175:512–518.